Available online at www.sciencedirect.com
SCIENCE DIRECT®
Agricultural and Forest Meteorology 116 (2003) 159–179
AGRICULTURAL AND FOREST METEOROLOGY
www.elsevier.com/locate/agrformet

Critical evaluation of micrometeorological methods for measuring ecosystem–atmosphere isotopic exchange of CO_2

David R. Bowling*, Diane E. Pataki, James R. Ehleringer

Department of Biology, University of Utah, 257 South 1400 East, Salt Lake City, UT 84112-0820, USA

Received 19 August 2002; received in revised form 5 January 2003; accepted 6 January 2003

Abstract

Isotopic net ecosystem exchange (isofluxes, or flux densities of $^{13}CO_2$) can be combined with standard eddy covariance methods to partition net ecosystem exchange of carbon dioxide (F) into its component one-way fluxes, photosynthesis and respiration. At present, the approaches used to estimate isotopic fluxes are labor-intensive and dependent on several assumptions. To assess the relative utility of the available methods, we studied an ecosystem associated with large CO_2 fluxes and maximal isotopic exchange. Three independent techniques were used to measure isotopic flux densities over an irrigated alfalfa field: (1) a combination of standard eddy covariance and flask sampling; (2) the flux-gradient method; and (3) hyperbolic relaxed eddy accumulation (HREA). Consistent isotopic flux results were obtained via the three methods, with similar diurnal patterns and peak midday isotopic flux densities of 600–700 $\mu mol\,m^{-2}\,s^{-1}$ ‰.

Air samples were collected over a wide range of CO_2 mole fractions (325.3–597.5 $\mu mol\,mol^{-1}$) and isotopic composition (−5.9 to −15.4‰). The relationship between isotopic composition ($\delta^{13}C$) and CO_2 mole fraction was consistent among types of samples, except for HREA samples during the morning boundary layer transition.

Total ecosystem respiration was estimated based on a regression against soil temperature, and the flux and isotopic flux measurements were used to examine whole-canopy photosynthetic discrimination (Δ_{canopy}) and the isotopic composition of the photosynthetic flux. Δ_{canopy} weighted by net ecosystem exchange was 17.9‰. The isotopic content of total ecosystem respiration, soil respiration, and foliar respiration, and $\delta^{13}C$ of various organic components (leaves, roots, soil organic matter) were examined and evaluated relative to Δ_{canopy}. The $\delta^{13}C$ of organic components does not appear to be a good predictor of $\delta^{13}C$ of ecosystem CO_2 fluxes.

Keywords: Net ecosystem exchange; Isotopic fluxes; Isoflux; Photosynthesis; Respiration; Hyperbolic relaxed eddy accumulation

1. Introduction

Stable isotopes of carbon dioxide provide a unique way to investigate aspects of the carbon cycle within terrestrial ecosystems. Uptake of atmospheric CO_2 by photosynthesis is associated with a change in the relative amounts of ^{13}C and ^{12}C. The $^{13}C/^{12}C$ isotope ratio of CO_2 in air (expressed as $\delta^{13}C$, in dimensionless "units" of ‰, Farquhar et al., 1989) is roughly −8‰ during the daytime, and $\delta^{13}C$ of C_3 plant materials and ecosystem components is −22 to −32‰. The process of photosynthesis removes relatively more of the lighter $^{12}CO_2$ isotope, and leaves the air enriched in the heavy $^{13}CO_2$ isotope ($\delta^{13}C$ of photosynthetic sugars is more negative than that of the air, and $\delta^{13}C$ of air becomes more positive during photosynthesis as the

* Corresponding author. Tel.: +1-801-581-2130; fax: +1-801-581-4665.
E-mail address: bowling@biology.utah.edu (D.R. Bowling).

0168-1923/03/$ – see front matter © 2003 Elsevier Science B.V. All rights reserved.
doi:10.1016/S0168-1923(03)00006-6

Nomenclature

a	intercept of a regression between $\delta^{13}C$ and $[CO_2]$ (‰)
b	HREA empirical coefficient
C	CO_2 mole fraction [ ] within the canopy ($\mu mol\,mol^{-1}$)
d	zero-plane vertical displacement height
F	net ecosystem exchange of CO_2 ($\mu mol\ CO_2\ m^{-2}\ s^{-1}$)
F_A	assimilation flux density of CO_2 ($\mu mol\ CO_2\ m^{-2}\ s^{-1}$)
F_c	flux density of CO_2 ($\mu mol\ CO_2\ m^{-2}\ s^{-1}$)
F_R	respiratory flux density of CO_2 ($\mu mol\ CO_2\ m^{-2}\ s^{-1}$)
F_{13}	net ecosystem exchange of $^{13}CO_2$ ($\mu mol\ ^{13}CO_2\ m^{-2}\ s^{-1}$)
F_δ	isoflux, analogous to net ecosystem exchange of $^{13}CO_2$, but expressed using δ notation ($\mu mol\ CO_2\ m^{-2}\ s^{-1}$ ‰)
G	soil heat flux density ($W\,m^{-2}$)
H	sensible heat flux density ($W\,m^{-2}$)
k	von Karman constant (dimensionless)
K	eddy diffusivity ($m^2\,s^{-1}$)
L	Obukhov length (m)
LE	latent heat flux density ($W\,m^{-2}$)
m	slope of a regression between $\delta^{13}C$ and $[CO_2]$ ($mol\,\mu mol^{-1}$ ‰)
R	molar ratio of heavy to light isotope ($^{13}C/^{12}C$)
R_n	net radiation flux density ($W\,m^{-2}$)
SOM	soil organic matter
T	temperature (°C)
u^*	friction velocity ($m\,s^{-1}$)
vpd	vapor saturation deficit of air (kPa)
w	vertical wind velocity ($m\,s^{-1}$)
z	height within the canopy (m)

Greek symbols

$\delta^{13}C$	carbon isotopic composition (‰)
$\delta^{18}O$	oxygen isotopic composition (‰)
Δ_{canopy}	whole-canopy, flux-weighted carbon isotope discrimination by photosynthesis (‰)
ρ	air density ($mol\,m^{-3}$)
σ_w	standard deviation of vertical wind velocity ($m\,s^{-1}$)
Φ	universal profile function (dimensionless)

Subscripts

a	air within the canopy
A, P	photosynthetic assimilation flux
c	flux of CO_2
dn	downdraft
R	respiration flux
R-branch	branch respiration flux
R-soil	soil respiration flux
up	updraft
1, 2	height 1 or 2

day progresses). Respiration then releases CO_2 back to the atmosphere which is ^{13}C depleted, causing the carbon isotope ratio of CO_2 in the atmosphere to decrease. As a result, there is significant diurnal variation in the isotopic content of CO_2 within terrestrial ecosystems (Keeling, 1958; Quay et al., 1989; Flanagan et al., 1996; Buchmann et al., 1997; Bowling et al., 1999a).

The isotopic composition of organic matter and of ecosystem CO_2 fluxes are roughly in balance, but can differ due to temporal separations in photosynthetic and respiratory activities or because of longer-term carbon dynamics. To date there is no definitive evidence of carbon isotope fractionation with mitochondrial respiration (Lin and Ehleringer, 1997). However, some authors define fractionation in different ways, leading to debate in the literature. Isolated leaf sugars can differ isotopically from CO_2 respired from those leaves (Duranceau et al., 1999; Ghashghaie et al., 2001), but it is difficult to establish the exact chemical substrate for leaf respiration. Plant secondary compounds do show systematic variation in isotopic composition (Gleixner et al., 1998), and preferential degradation of organic compounds in plant respiration or microbial oxidation might lead to isotopic differences in the bulk organic substrate and respired CO_2 (e.g. Ehleringer et al., 2000). There is some evidence of isotopic changes upon fungal uptake of sugars (Henn and Chapela, 2000), but in an ecosystem context such apparent fractionations could not be sustained indefinitely and still conserve mass.

Total ecosystem respiration is always depleted (more negative $\delta^{13}C$) in ^{13}C relative to the air, and photosynthesis always leaves the air more enriched. These labels mean that the ecosystem-scale processes of photosynthesis and respiration can be studied by examination of the isotopic content of CO_2 in terrestrial ecosystems (Yakir and Wang, 1996; Lloyd et al., 1996; Flanagan et al., 1996; Bowling et al., 2001b).

2. The challenge of measuring isotopic fluxes

Yakir and Wang (1996) were the first to exploit isotopic CO_2 flux variation in a micrometeorological context. They used isotopic fluxes to separate net ecosystem exchange of CO_2 (F) into its gross one-way component fluxes, ecosystem respiration and photosynthesis, in wheat, cotton, and corn crops. Simultaneously, Lloyd et al. (1996) derived a useful suite of equations that have been used to investigate isotopic fluxes of CO_2 within ecosystems (Lloyd et al., 1996; Flanagan et al., 1997) and at the regional scale (Lloyd et al., 2001). Bowling et al. (2001b) extended these studies with:

$$F = F_R + F_A, \tag{1}$$

$$F_\delta = (\delta^{13}C_R)F_R + (\delta^{13}C_a - \Delta_{canopy})F_A. \tag{2}$$

The notation in Eqs. (1) and (2) is consistent with Appendix A, and differs slightly from Bowling et al. (2001b). These equations were initially derived with the intention of using F and isotopic flux measurements (isoflux, F_δ) to solve for total ecosystem respiration (F_R) and net photosynthetic assimilation (F_A). F_δ is conceptually identical to the net ecosystem exchange of $^{13}CO_2$, but there is an important mathematical distinction, described in detail in Appendix A. Solving Eqs. (1) and (2) for F_R and F_A requires a priori specification of: (1) the isotope ratio of total ecosystem respiration ($\delta^{13}C_R$); (2) the isotope ratio of atmospheric CO_2 ($\delta^{13}C_a$); and (3) whole-canopy integrated photosynthetic carbon isotope discrimination (Δ_{canopy}). Since this definition of Δ_{canopy} is based on leaf-level net discrimination (defined as isotopic fractionation during net carbon assimilation, which is defined as gross leaf carbon uptake minus leaf respiration), we must include foliar respiration in the assimilation flux during the day (F_A) and in the respiration flux at night (F_R) (Lloyd et al., 1996; Bowling et al., 2001b).

Ideally, F_δ could be measured directly via eddy covariance of $^{13}CO_2$, and appropriate characterization of the isotopic storage flux. The former would require a field-based instrument that can accurately measure $^{13}CO_2$ mole fractions at a sampling interval on the order of 100 ms, with considerable precision (corresponding to an isotope ratio of 0.05‰). In this regard, there are several promising spectroscopic technologies. These include tunable diode lasers (TDL, Becker et al., 1992), a combination of TDL with cavity ringdown spectroscopy (Crosson et al., 2002), and Fourier-transform infrared spectroscopy (Esler et al., 2000). At present no instruments meet these requirements, and we are limited to three indirect methods for assessing F_δ at the ecosystem-scale. These are the flux-gradient technique (Yakir and Wang, 1996), hyperbolic relaxed eddy accumulation (Bowling et al., 1999b), and a combination of eddy covariance and flask sampling called the EC/flask technique (Bowling et al., 2001b).

The **flux-gradient** or **gradient profile** technique (e.g. Businger, 1986) relates a vertical gradient of an atmospheric constituent (such as CO_2) to a flux via:

$$F_c = \rho K \frac{C_1 - C_2}{z_1 - z_2}, \tag{3}$$

where F_c is the flux of interest, ρ the air density, and C_1 and C_2 the CO_2 mole fractions at two heights, z_1 and z_2. K is an empirical parameter called the eddy diffusivity, and can be determined by measurements of the vertical wind profile, Monin–Obukhov similarity theory, or by assuming similarity with another scalar that can be measured via eddy covariance (sensible heat, water vapor, etc.) and rearranging Eq. (3). This equation can be modified for $^{13}CO_2$ flux by multiplying each mole fraction or flux term by the isotope ratio of CO_2 at that height:

$$\delta_c F_c = \rho K \frac{(\delta^{13}C_1)C_1 - (\delta^{13}C_2)C_2}{z_1 - z_2}. \tag{4}$$

Thus, the isotopic flux ($\delta_c F_c$) can be determined by measuring $\delta^{13}C$ and $[CO_2]$ (where [ ] denotes mole fraction) at two heights above a plant canopy, and samples can be returned to a laboratory for analysis on any time scale. The gradient method is attractive for its simplicity. Further, K can be determined entirely

independently of the $\delta^{13}C$ and $[CO_2]$ measurements. (As with net ecosystem exchange, the isotopic flux $\delta_c F_c$ must be combined with an isotopic storage flux to produce F_δ in Eq. (2)—see Appendix A for details.)

The gradient technique assumes that mole fraction variation in the atmosphere follows well-defined vertical profiles. Such profiles are observed only in the surface layer, which above a rough plant canopy can extend many (5–10) canopy heights above the canopy top. In the roughness sublayer, and within the canopy itself, serious problems with this technique emerge (Raupach, 1979; Cellier and Brunet, 1992), and fluxes can even be in a direction opposite the observed mole fraction gradient (Denmead and Bradley, 1985). In practice, this restricts use of the gradient method to sites such as crops and grasslands that are aerodynamically smooth and short-statured.

To develop a method that could be used to estimate isotopic fluxes over forests, Bowling et al. (1999b) merged the relaxed eddy accumulation technique (Businger and Oncley, 1990) with hyperbolic hole analysis (Shaw, 1985) to produce the **hyperbolic relaxed eddy accumulation** (HREA) method. This method relates the flux to mole fraction differences in updrafts (C_{up}) and downdrafts (C_{dn}) via:

$$F_c = \rho b \sigma_w (C_{up} - C_{dn}), \quad (5)$$

where σ_w is the standard deviation of the vertical wind velocity and b an empirical coefficient. Sampling decisions are made every 100 ms and samples are collected in updraft or downdraft containers, or discarded. Samples are accumulated in the containers over a 30–45 min time period and then the bulk sample is analyzed at leisure. Eq. (5) can be extended for isotopic fluxes as:

$$\delta_c F_c = \rho b \sigma_w ((\delta^{13}C_{up}) C_{up} - (\delta^{13}C_{dn}) C_{dn}), \quad (6)$$

where $\delta^{13}C_{up}$ and $\delta^{13}C_{dn}$ are the carbon isotope ratios of updrafts and downdrafts. In HREA, only updrafts and downdrafts exceeding a certain threshold are sampled, and their identification is dependent on measurements of wind and $[CO_2]$ (Bowling et al., 1999a,b).

While this technique provides maximal isotopic differences in updrafts and downdrafts, it suffers from several problems. One disadvantage of HREA is that the majority of air (80%) is discarded, and roughly 10% of the original volume is sampled into each of the updraft and downdraft containers. The "information" contained in the discarded air must be reconstructed through the b coefficient. The determination of b is problematic—this has been done by assuming similarity with $[CO_2]$, measuring $[CO_2]$ in updrafts and downdrafts, and CO_2 flux by eddy covariance, and rearranging Eq. (5) to solve for b (Bowling et al., 1999a). This is somewhat circular; if the eddy covariance fluxes (F_c) are used to determine the isotopic flux (i.e. if the HREA fluxes are calculated using b derived from eddy covariance), and then F and F_δ are used together (Eqs. (1) and (2)), then they are not strictly independent. Further, determining b in this fashion assumes that CO_2 and $^{13}CO_2$ act identically in the atmosphere, which is likely false when there are major differences in sources and sinks (such as in a forest with photosynthesis and respiration occurring). A recent examination of this and other conditional-sampling techniques by Ruppert (2002) showed that under some conditions large errors can result from violations of scalar similarity using HREA.

The simplest of the methods to determine isotopic fluxes, which we will refer to as the **EC/flask** technique, involves establishing a regression between $\delta^{13}C$ and $[CO_2]$, then using this regression combined with 10 Hz measurements of $[CO_2]$ to calculate $^{13}CO_2$ flux via:

$$\delta_c F_c = \rho \overline{w'[(\delta^{13}C_a) C_a]'} = \rho \overline{w'[(mC_a + a) C_a]'}, \quad (7)$$

where w is vertical wind velocity, m and a the slope and intercept of the regression $\delta^{13}C_a = mC_a + a$, and overbars denote Reynolds averaging, and primes denote deviation from that average. The EC/flask method has been described in detail elsewhere (Bowling et al., 1999a, 2001b). It has the major advantage that the only measurements required beyond standard eddy flux instrumentation are flask samples of $\delta^{13}C$ and $[CO_2]$ in air. Isotopic flux studies are too few at present to firmly establish just how frequently these samples need to be collected, but there can be important ecophysiological variation in $\delta^{13}C_R$ on a time scale of days to weeks (Buchmann et al., 1997; Bowling et al., 2002; Ometto et al., 2002), which is likely a good proxy.

A disadvantage of the EC/flask technique is that it assumes a regression between $\delta^{13}C$ and $[CO_2]$ is valid at all time scales associated with turbulent exchange (100 ms to 30 min, or longer), but the regression is established with flask samples collected relatively slowly. Bowling et al. (2001b) showed that

Table 1
Geometric mean regressions of $\delta^{13}C$ vs. $1/[CO_2]$ and $\delta^{13}C$ vs. $[CO_2]$ (last row only)

Sample type	Intercept	Slope	r^2	n
EC/flask	−26.60 ± 0.12	6757.3 ± 49.0	1.00	19
Gradient	−26.63 ± 0.37	6834.5 ± 142.1	0.98	42
HREA	−26.90 ± 0.13	6916.6 ± 52.6	1.00	59
EC/flask and gradient, nocturnal[a]	−27.12 ± 0.17	7026.6 ± 75.4	1.00	27
Soil	−24.73 ± 0.46	5998.3 ± 195.6	0.98	20
Branch	−23.79 ± 0.50	5759.6 ± 247.3	0.98	14
EC/flask[b]	6.62 ± 0.29	−0.040 ± 0.001	0.98	61

Errors are presented as the standard error of the slope or intercept.
[a] Regression used to calculate $\delta^{13}C_R$ and $\delta^{13}C_a$.
[b] Regression used to calculate EC/flask fluxes.

this may not be a problem for samples collected over time scales varying from 500 ms to 30 min. A more serious issue is the choice of a regression of $\delta^{13}C$ versus $[CO_2]$ instead of $\delta^{13}C$ versus $1/[CO_2]$ (Keeling, 1958). Both are satisfactory in predicting isotope ratio variation based on $[CO_2]$ in the range 330–500 μmol mol^{-1}, but only the latter matches observations at higher CO_2 values (see Fig. 4 and Table 1). However, on a theoretical basis, Bowling et al. (2001b) argued that using the Keeling relationship in Eq. (7) ($m_2/C_a + a_2$ instead of $mC_a + a$) forces isotopic equilibrium (where $\delta^{13}C_R = \delta^{13}C_a - \Delta_{canopy}$ in Eq. (2)). In this case Eq. (2) becomes a multiple of Eq. (1), and there is no unique information in $^{13}CO_2$ that is not already contained in CO_2 fluxes. Ecosystems seem to operate very near the condition of isotopic equilibrium; thus, indirect empirical techniques such as this one should be examined quite critically.

Clearly, each of these indirect methods has advantages and disadvantages. The goal of the present study was to investigate their relative merits in an ecosystem that would provide large isotopic signals. We first describe the measurements in detail, then apply the equations to calculate Δ_{canopy}, and evaluate this estimate of whole-canopy photosynthetic discrimination by comparison with observed isotopic variation in various ecosystem organic components and fluxes.

3. Methods

3.1. Site

This study was conducted in an irrigated field of alfalfa (*Medicago sativa* L.) in the Cache Valley, Utah (41°53′N, 111°50′W, 1380 m elevation) between 11 and 25 August 2000. Since a land-use history of C_4 crops would confound our isotopic measurements, we selected a site that contained strictly C_3 plants for more than 20 years. The site was flat and measured 400 m × 400 m (16 ha in area). Following local agricultural practice, the field was heavily irrigated roughly 2 weeks prior to measurements and not irrigated again. Rain fell during a single afternoon (23 August), otherwise the weather was sunny, hot, and dry.

3.2. Eddy covariance and meteorology

Fluxes of sensible heat, latent heat, and carbon dioxide were measured using the eddy covariance technique at a height equal to three canopy heights ($3h$, where $h = 54.8 \pm 12.6$ cm on 24 August). Instrumentation included an open-path infrared gas analyzer (LI-7500, Licor Inc., Lincoln, NE) and a sonic anemometer (CSAT3, Campbell Scientific Inc., Logan, UT). Fluxes were averaged over 30 min periods, and standard corrections for density were applied (Webb et al., 1980). Data were examined for stationarity by comparing 5 and 30 min covariances—if the mean of the six 5 min w-CO_2 covariances differed from the 30 min covariance by more than 30%, the flux data were excluded from some analyses (Foken and Wichura, 1996). CO_2 mole fraction was measured at several heights ($5h$, $3h$, $0.8h$, $0.5h$, and $0.05h$) using a second IRGA (LI-6262, Licor Inc., Lincoln, NE), and used to compute the storage component of F (Wofsy et al., 1993). All CO_2 measurements in this study are referenced to WMO $[CO_2]$ standards.

3.3. Isotopic fluxes

Isotopic fluxes of $^{13}CO_2$ were measured using the EC/flask technique, the flux-gradient technique, and hyperbolic relaxed eddy accumulation. While the method of sampling in each flux measurement technique differed, in all cases the samples were ultimately stored in 100 ml glass flasks (34–5671, Kontes Glass Co., Vineland, NJ) in the field and then analyzed in our laboratory. Carbon isotope ratios of CO_2 in the flasks were measured using a continuous flow isotope ratio mass spectrometer (IRMS, Finnigan DELTAplus, Finnigan MAT, San Jose, CA), as described by Ehleringer and Cook (1998). Precision for $\delta^{13}C$ was determined daily by comparison to known standards and was typically ±0.15‰. Corrections for the presence of ^{17}O were applied, and CO_2 was separated from N_2O by gas chromatography before analysis. We report all carbon isotope ratio values in this paper relative to the international PDB standard. [CO_2] was measured using the bellows/IRGA technique of Bowling et al. (2001a) with a precision of 0.3 μmol mol^{-1}. Isotopic storage fluxes were calculated from the [CO_2] profile measurements and the relation between $\delta^{13}C$ and [CO_2] as described by Bowling et al. (2001b); however, due to the small air volume below our flux measurement height the storage components of F and F_δ were negligible.

3.3.1. EC/flask

We established the relationship between $\delta^{13}C$ and [CO_2] using samples collected over a range of time periods, both at night and during the day. Nineteen samples (which we denote EC/flask samples) were collected in 100 ml flasks by pulling air at 1000 ml min^{-1} through a $Mg(ClO_4)_2$ trap to remove water vapor with a pump (UNMP50KNDC, KNF Neuberger Inc., Trenton, NJ) downstream of the flask. These were collected at a variety of heights (5h, 3h, 0.8h, 0.5h, and 0.05h) within the canopy, with the intention of maximizing the range of [CO_2] in the samples (which minimizes the standard error of the Keeling intercept, Pataki et al., 2003). The EC/flask samples were combined with 42 gradient samples (described below) and a geometric mean regression of $\delta^{13}C$ versus [CO_2] was performed (Table 1). This regression was used to compute isotopic fluxes via Eq. (7).

3.3.2. Flux-gradient

We collected air samples every 4 h (except at 2 a.m.) over a 5-day period (20–24 August) at two heights (3h and 5h). These heights were intentionally chosen above the roughness sublayer to avoid complications associated with counter-gradient fluxes. Air was pumped from the two sampling heights through 10.4 l glass buffer volumes at 347 ml min^{-1} to provide a 30 min residence time in the buffers. The air was dried using $Mg(ClO_4)_2$, and pulled through a 100 ml sampling flask via a diaphragm pump downstream of the flask.

Gradient isotopic fluxes were calculated using Eq. (4), and the eddy diffusivity for CO_2 (K) was computed from Monin–Obukhov similarity theory via:

$$K = \frac{ku^*(z - \mathrm{d})}{\Phi}, \tag{8}$$

$$\Phi = \begin{cases} \left(1 + 16\left|\dfrac{z-\mathrm{d}}{L}\right|\right)^{-1/2}, & -2 \le \dfrac{z-\mathrm{d}}{L} \le 0, \\ 1 + 5\left(\dfrac{z-\mathrm{d}}{L}\right), & 0 < \dfrac{z-\mathrm{d}}{L} \le 1, \end{cases} \tag{9}$$

where k is von Karman's constant, u^* the friction velocity, z the measurement height, d the zero-plane displacement height, Φ is the universal function describing scalar profiles as a function of the stability parameter $(z-d)/L$, and L the Obukhov length (Raupach, 1979; Kaimal and Finnigan, 1994). Implicit in this approach is the assumption that the eddy diffusivities for momentum and scalars are identical (i.e. the turbulent Schmidt number equals unity). Flesch et al. (2002) suggest that the Schmidt number can be smaller (0.6 on average in their study), which would cause our gradient CO_2 measurements to underestimate the true flux.

3.3.3. HREA

The HREA method has been used once before with a sampling system involving cryogenic purification of CO_2 during sample collection (Bowling et al., 1999a). For the present study, we used a much simpler system involving flexible bags as collection reservoirs (Fig. 1). Since the simplified technique is more practical, we describe our new design in detail here. It

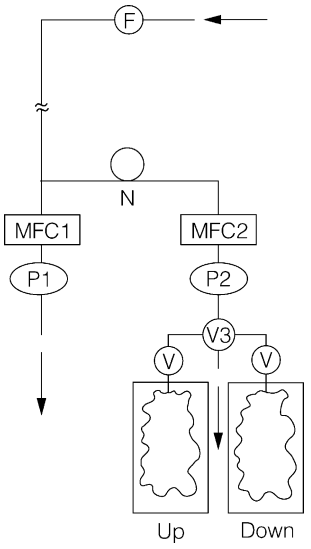

Fig. 1. Schematic diagram of the HREA system.

is similar in design to the relaxed eddy accumulation systems of Oncley et al. (1993) and Bowling et al. (1998). HREA sampling decisions, based on 10 Hz wind and CO_2 measurements, were made as described by Bowling et al. (1999a). We used an asymmetric hyperbolic threshold of 1.1, and a recursive filter (McMillen, 1988) to estimate relevant turbulent parameters (w', σ_w, CO_2', σ_{CO_2}). These parameters are described in detail in other papers (Bowling et al., 1999a,b). HREA isotopic fluxes were calculated according to Eq. (6).

Air was drawn (Fig. 1) from within 10 cm of the sonic anemometer path at 5000 ml min^{-1} through a primary flow path consisting of 25 cm × 0.64 cm o.d. stainless steel tubing, a 15 μm sintered ceramic filter (F, SS-4FW-15, Swagelok/NUPRO Co., Willoughby, OH), 7 m of polymer tubing (0.64 cm o.d., Dekoron, Synflex Specialty Products, Mantua, OH), and a mass flow controller (MFC1, 1179A, MKS Instruments, Andover, MA) by two pumps in parallel (P1, PC-X76-001/7, Charles Austen Pumps Ltd., Surrey, UK). A subsample of this airstream was drawn at 620 ml min^{-1} through a Nafion counterflow drying membrane (MD-070-48S, Perma-Pure Inc., Toms River, NJ) to remove water vapor, and a second mass flow controller (MFC2, 1179A, MKS Instruments, Andover, MA) by a pump (P2, UNMP50KNDC, KNF Neuberger Inc., Trenton, NJ). Downstream of the pump (P2) the flow was routed via a three-way Teflon manifold valve (V3, P-01367-81, Cole-Parmer Instrument Co., Vernon Hills, IL) into updraft/downdraft bags or vented.

Internal volume of various system components was measured manometrically in the lab and the appropriate delay (2.3 s) applied to valve control signals to synchronize an event at the sonic/IRGA to the associated plumbing change. Flow rate in the longer (7 m) sampling line (5620 ml min^{-1}) was sufficient to maintain turbulent flow (Reynolds number = 2466), but flow in the shorter secondary path (tens of cm in length) was laminar.

The bags (party balloons, Anagram International Inc., Minneapolis, MN) were flexible and made of four layers, which (from the inside) were polyethylene, nylon, aluminum flake, and ink. The bags were sealed after collection using stainless steel toggle valves (V, SS-1GS4, Swagelok/Whitey Co., Highland Heights, OH). Stainless steel filler tubes (25 cm × 0.64 cm o.d.) were drilled with multiple holes and inserted into the flexible valves on the bags and sealed with rubber bands. Bags were flushed with dried ambient air and pumped flat immediately prior to filling. Samples were collected over 30 min then the samples were immediately transferred to 100 ml glass flasks and stored until analysis. Samples did not reside in the bags for more than 35 min.

Several laboratory tests were performed to assess the integrity of gas samples stored in the bags. Results of some of these tests are shown in Table 2. Air from a compressed cylinder with known isotope ratio was introduced into the bags. Some samples were immediately transferred to flasks (0 min), and others sat

Table 2
Results of tests of isotopic integrity in the HREA sampling bags

Time in bag (min)	$\delta^{13}C$ (‰)	$\delta^{18}O$ (‰)	n
0	−30.48 ± 0.05	−0.56 ± 0.06	11
30	−30.48 ± 0.08	−0.18 ± 0.16	10
60	−30.47 ± 0.09	0.10 ± 0.33	4
122	−30.35	1.89	1
240	−30.29	3.02	1
955	−30.09	8.92	1
1800	−30.12 ± 0.13	14.00 ± 2.37	4

Shown are carbon and oxygen isotope ratios of CO_2 in air samples that were put into bags and immediately transferred to flasks (0 min), or after samples aged in bags for increasing time periods.

in bags for varying periods of time, up to 30 h. After aging, samples were transferred to pre-evacuated 1.7 l glass flasks, the CO_2 was purified cryogenically under vacuum, and analyzed via dual inlet mass spectrometry (Finnigan MAT 252, Finnigan, San Jose, CA). A shift in both $\delta^{13}C$ and $\delta^{18}O$ of CO_2 was apparent over time (Table 2), but within a 60 min time period the shift in $\delta^{13}C$ was insignificant. Tests were also performed with the full HREA system as it was used in the field, using dry and humidified compressed air of known isotope ratio, with similar results (not shown).

There was an immediate change in $\delta^{18}O$ measured in the bags that increased dramatically over time (Table 2). We attempted to identify the cause of this shift without success. Based on these results, we do not recommend using these bags to collect samples that will be analyzed for $\delta^{18}O$ of CO_2; at present, the cryogenic system of Bowling et al. (1999a) is the only alternative for HREA sampling with oxygen isotopes of CO_2. However, recent tests in other laboratories have shown promising results with $\delta^{13}C$ and $\delta^{18}O$ in bags after they have been conditioned (Ruppert and Brand, Max-Planck-Institut für Biogeochemie, personal communication).

3.4. Soil respiration rate

Fourteen PVC collars were installed every 7 m along a 100 m transect on 19 August. Each collar measured 9.5 cm in diameter and was inserted to 5 cm soil depth. Collars were installed in small patches of bare soil between aboveground plant parts, immediately adjacent to the stems. Aboveground plant components were excluded from the chambers. Respiration rates were measured using a portable photosynthesis system (LI-6200, Licor Inc., Lincoln, NE) with a 960 ml soil chamber (6000-09, Licor Inc.) configured in a closed loop, by examining the rate of a 20 μmol mol^{-1} change in [CO_2] over roughly 1 min. Due to an undetected probe malfunction during the experiment, soil temperature data measured concomitantly at each chamber were unreliable. We present soil temperature data measured at a central location along the transect using a Cu–Co thermocouple at 0.04 m depth (5 s data averaged every 30 min). This is not necessarily the most appropriate depth for this crop if most respiration occurs in deeper roots, but is a suitable indicator of the diurnal pattern.

3.5. $\delta^{13}C$ of ecosystem respiration

The intercept of a geometric mean regression between $\delta^{13}C$ and 1/[CO_2] (a Keeling plot) was used on nocturnal EC/flask and gradient samples (Table 1) to calculate $\delta^{13}C_R$, the isotope ratio of ecosystem respiration (Keeling, 1958). Outliers were selected and removed as necessary as described by Bowling et al. (2002).

3.6. Calculation of Δ_{canopy}

F_R was prescribed as a function of soil temperature, and Eqs. (1) and (2) were solved for F_A and Δ_{canopy}. For this analysis, F and F_δ were measured using eddy covariance and the EC/flask technique, respectively, with appropriate storage fluxes included. $\delta^{13}C_R$ was derived from a Keeling plot as described above, and $\delta^{13}C_a$ was calculated from the Keeling regression (Table 1) and measured [CO_2] at 0.4 m height (0.8h). We then compared this estimate of Δ_{canopy} to isotopic content of ecosystem organic components and respired CO_2.

3.7. $\delta^{13}C$ of leaves, roots, and soil organic matter

Sun leaf samples were saved from the plants used for foliar respiration measurements (described below). Bulk soil and root samples were collected from three separate pits at depths of 4, 9, 20, and 32 cm in thin (2 cm) layers. All organic samples were dried to constant mass at 60 °C. Roots were removed from soil samples and tap roots and fine roots (<2 mm diameter) saved. Root-free soil samples were acid-washed to remove carbonates (0.5N HCl). Leaves, roots, and bulk soil were ground with mortar and pestle to #20 mesh and subsamples (2 mg leaf and root, 20 mg soil) were flash-combusted and analyzed for $\delta^{13}C$ on an IRMS (deltaS, Finnigan MAT, San Jose, CA). Measurement precision was 0.2‰, and data are presented as means and standard errors of three or more replicates.

3.8. $\delta^{13}C$ of foliar respiration

On the evening of 22 August, measurements of the isotope ratio of foliar respiration were made. This was done by adding an assembly of five 100 ml flasks (connected to each other in parallel) to the closed loop soil

respiration chamber. The chamber was used simply as a gas-exchange enclosure to insert detached foliar components. First, all flask stopcocks were opened, and the pump run for several minutes to fill the flasks with ambient air near the ground. Next, the plastic protective cap for the soil respiration chamber was attached, and the empty chamber and flask assembly were flushed for several minutes, to fully mix the internal volume. Next, the pump was turned off, and three to five alfalfa stems, roughly 60 cm long, were excised at the base of the plants, inserted into the chamber, and immediately the cap was replaced and the pump turned on. Attention was paid to avoid contaminating the sample with human breath. As the excised stems and leaves respired, [CO_2] increased in the chamber and was monitored using the LI-6200. In roughly 50 ppm increments, the stopcocks were closed on individual flasks. This provided a set of five flasks per measurement, collected over several minutes, with [CO_2] varying from near ambient at the start to 200 ppm above ambient at the end of the measurement. In total, five replicate measurements were made (five different foliage samples) between 21:00 and 22:00 h local time. All foliar measurements were pooled together and a single Keeling plot was constructed for the set (Table 1).

3.9. $\delta^{13}C$ of soil respiration

On 22 August, at 16:00–18:00 h local time, estimates of the isotope ratio of soil-respired CO_2 were made. The procedure was identical to that for the foliar measurements, except that once the empty chamber and flask assembly was flushed and mixed, the cap was removed and the chamber gently placed on one of the soil respiration collars. As [CO_2] increased in the system, flasks were closed in 50 ppm increments. Five chambers were measured in total, and a single Keeling plot was constructed (Table 1). A single measurement of five flasks was completed in several minutes.

4. Results and discussion

4.1. Energy and CO_2 fluxes

A major limitation of isotopic flux studies to date has been a lack of sampling frequency. Typically only a few days of measurements are possible even with considerable effort (Yakir and Wang, 1996; Bowling et al., 1999a, 2001b). For this reason, we present as much data as possible. The alfalfa crop exhibited rapid growth during the 15 days (11–25 August) of our measurements, with mean canopy height changing from 34 to 55 cm. Isotopic fluxes were measured using the EC/flask technique on all 15 days, but due to labor and analytical requirements, the gradient and HREA methods were only employed during 20–24 August. We were concerned that fluxes at the beginning of this time period might be markedly different from the end, so we present data for the entire period as well as the 5-day subset when all isotopic techniques were used.

Energy fluxes are shown in Fig. 2. Available energy (the difference between net radiation (R_n) and soil heat flux (G)) was consistent over the 15 days. Latent heat (LE) fluxes (Fig. 2B) showed little day to day variation and closely followed available energy. Sensible heat fluxes (H), however, showed a contrast in diurnal pattern, with a negligible mid-morning peak and downward (negative) flux during the afternoon. The direction of flux was confirmed by independent measurements of air temperature at the two flux-gradient heights (data not shown), and prevented us from using those temperature measurements and H to compute the eddy diffusivity for CO_2 (as is common with the flux-gradient technique). The pattern of negative afternoon H has been observed by others, where irrigated and aerodynamically smooth crops in hot dry climates can transpire more energy as latent heat than is available as incoming radiation (Brakke et al., 1978; Rosenberg and Verma, 1978). This suggests that substantial horizontal advection of energy as sensible heat flux occurred at our site from the surrounding area.

Net ecosystem exchange (F) of CO_2 is shown in Fig. 3. Peak carbon uptake of -25 to $-30\ \mu mol\ m^{-2}\ s^{-1}$ occurred at about 12:30 h local time, which is earlier than the R_n and LE peaks at 13:00 and 14:00 h, respectively. These peak values of F are similar to other alfalfa studies reported (Verma and Rosenberg, 1976; Asseng and Hsiao, 2000). We observed no discernible difference in the fluxes measured over the 15-day period and the 5-day subset. Nocturnal respiration was higher in the evening than in the morning (see the line in Fig. 3), which is consistent with measured air and soil temperatures (not shown).

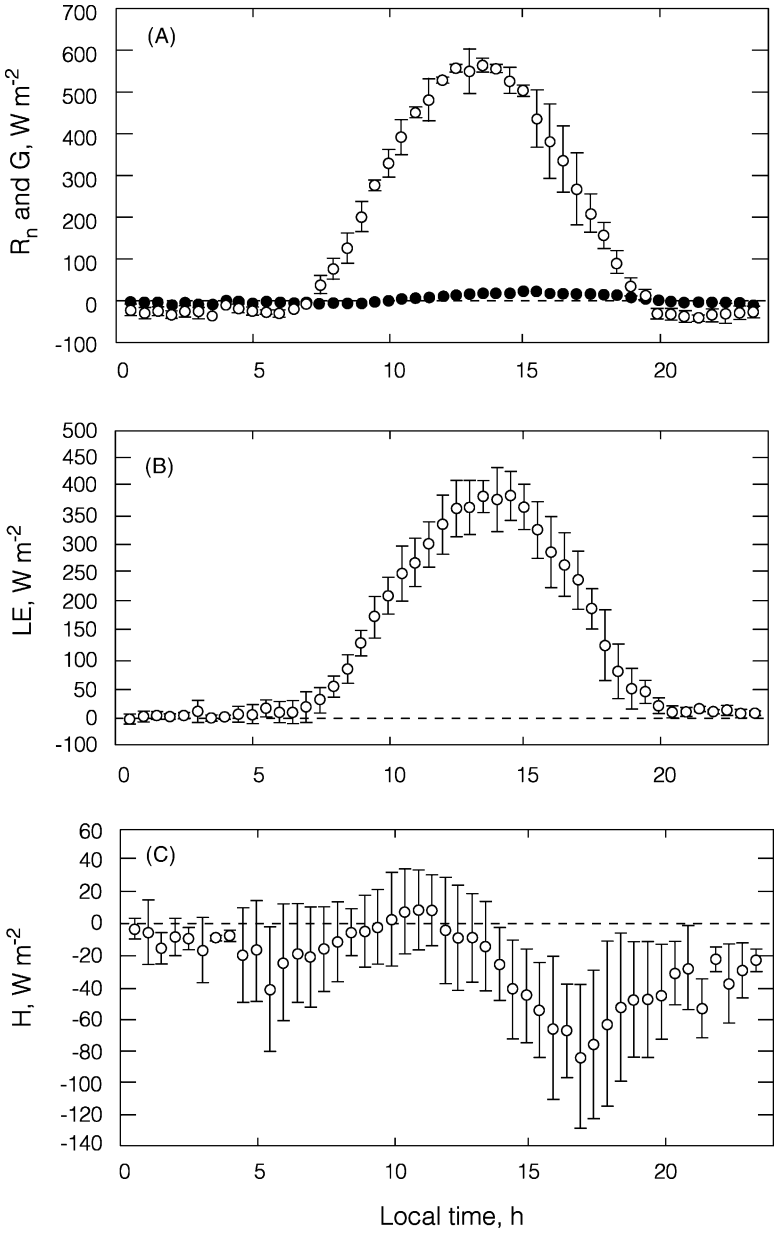

Fig. 2. Diurnal pattern of: (A) net radiation (empty circles) and soil heat flux (filled circles); (B) latent heat; and (C) sensible heat fluxes. Note the *y*-axis scales differ. Data are means and standard deviations of data during stationary periods from 11 to 25 August. Our sign convention is that non-radiative fluxes are positive when directed away from the canopy.

4.1.1. Isotopic relationships and fluxes

The relationship between $\delta^{13}C$ and [CO_2] was generally consistent among the various types of samples (Fig. 4). Flask air samples were obtained at midday with [CO_2] as low as 325.3 μmol mol^{-1}, which is evidence of strong photosynthetic removal of CO_2 within the canopy. Such low values represent a maximal isotopic signal associated with photosynthetic enrichment of canopy air ($\delta^{13}C$ was −5.9‰ at 325.3 μmol mol^{-1}). Similarly extreme values have been reported in alfalfa

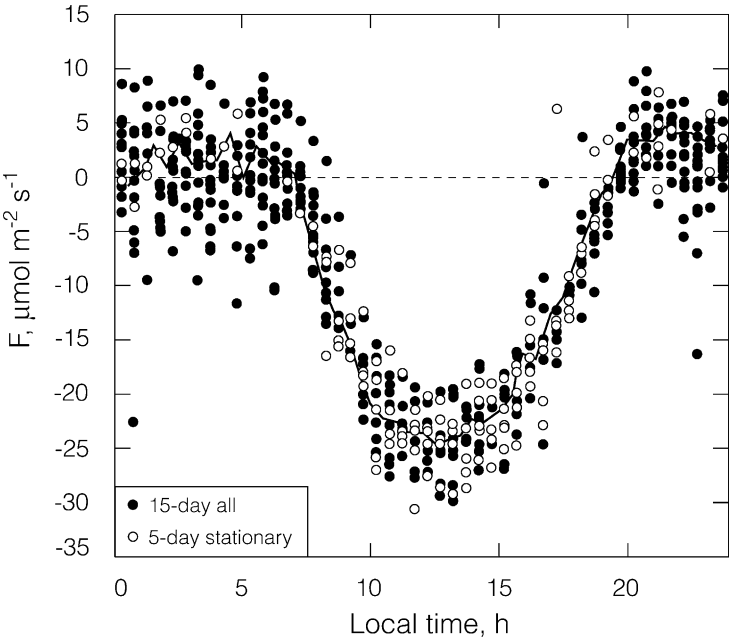

Fig. 3. Diurnal pattern of net ecosystem exchange of CO_2. Data are shown for all measurement periods from 11 to 25 August (filled circles), and for stationary periods only during 20–24 August (empty circles) for comparison. The latter period coincided with isotopic flux measurements. The line represents the stationary ensemble mean of all 15 days.

and corn crops by Buchmann and Ehleringer (1998). Midday minimum [CO_2] values differed strongly with height, with lowest mean (±S.D.) values of $321.2 \pm 5.9\,\mu mol\,mol^{-1}$, at 0.5*h* canopy heights, and higher ones above the canopy, $353.0 \pm 3.2\,\mu mol\,mol^{-1}$ at 5.0*h* (data not shown). These are substantially lower than background CO_2 at this latitude. (The Niwot Ridge, CO monthly means during August 2000 were $367.6\,\mu mol\,mol^{-1}$ and −7.92‰; data from NOAA/CMDL website: http://www.noaa.cmdl.gov.) High [CO_2] ($597.5\,\mu mol\,mol^{-1}$) and very negative $\delta^{13}C$ (−15.4‰) were observed in nocturnal samples, indicating respiratory buildup of carbon dioxide that was depleted in ^{13}C. The ranges in $\delta^{13}C$ observed in our study are among the highest ever reported.

Bowling et al. (1999a) reported a difference in the slopes of the $\delta^{13}C$ versus [CO_2] relationship between whole-air samples and HREA samples (updrafts or downdrafts), and suggested the difference was possibly due to differing time scales associated with the sampling strategies of each method. HREA samples consist of 100 ms air samples representing extreme updrafts and downdrafts that are accumulated over time. Bowling et al. (2001b) showed that whole-air samples collected over varying time periods (500 ms to 30 min) did not differ in their slopes, leaving the cause of the difference still unresolved. All samples analyzed for isotopic content are shown in Fig. 4, and these were collected over the entire diel cycle. The majority of samples showed a consistent pattern, but all HREA samples collected during the time period when the nocturnal boundary layer is breaking up (8:00 h local time) deviated from this pattern in a more positive isotopic direction (Fig. 4). We have no reason to suspect an experimental artifact unique to this sampling time period.

Although the 08:00 h HREA samples show a different slope than the rest, this pattern is not the same one reported by Bowling et al. (1999a), where all HREA samples on a given day fell on a common line. In the present study, all the morning boundary layer transition HREA samples fall on a common line, but other HREA samples are more consistent with whole-air samples. There are two possible reasons for this observation. First, high photosynthetic discrimination during the very early morning combined with

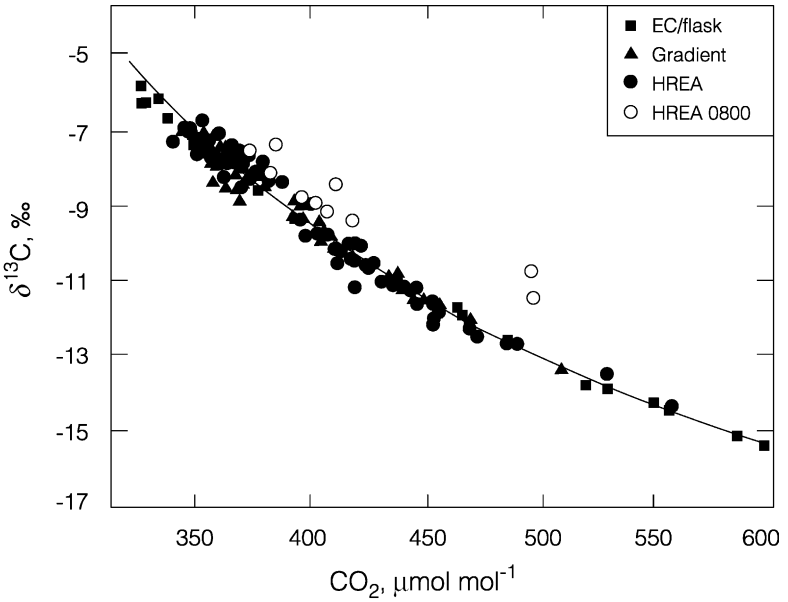

Fig. 4. The relationship between $\delta^{13}C$ and CO_2 for samples associated with the EC/flask (filled squares), flux-gradient (filled triangles), and HREA (filled circles) isotopic flux measurement techniques. The former two types represent whole-air samples, while the HREA are updraft or downdraft samples. HREA samples collected during the morning boundary layer transition (08:00–08:30 h local time, empty circles) are plotted separately. The line represents the Keeling relationship for nocturnal EC/flask and gradient samples ($\delta^{13}C = 7026.6/[CO_2] - 27.12$‰; Table 1).

very negative $\delta^{13}C_a$ due to respiratory buildup might cause substantial enrichment of above-canopy air relative to the normal mixing line, since the photosynthetic flux would have a very negative isotope ratio (Eq. (2), $\delta^{13}C_a - \Delta_{canopy}$). If so, this should be observed in whole-air samples as well. Unfortunately no gradient or EC/flask samples were collected during this time period for comparison. Second, the shallower slope is indicative of a lower discrimination relationship in general, consistent with some contribution from C_4 photosynthesis. It is possible that corn crops growing in the Cache Valley may have some influence that is apparent during the period of rapid boundary layer growth.

Measured isotopic fluxes are shown in Fig. 5A, including both stationary and non-stationary periods. Midday F_δ peaked at 600–700 µmol m^{-2} s^{-1} ‰, and nighttime values roughly averaged −100 µmol m^{-2} s^{-1} ‰. These values are similar to those reported over a deciduous forest in Tennessee (Bowling et al., 1999a, 2001b). Isotopic fluxes measured by the three methods were consistent in both diurnal pattern and magnitude, particularly when stationary atmospheric conditions were present (Fig. 5B). At night, there was a tendency for the gradient technique to overestimate F_δ relative to the others (Fig. 5A). However, we do not expect either the HREA or gradient techniques to be especially robust at night. The assumptions on which these methods are based are likely to fail within a neutral or stable nocturnal boundary layer.

4.1.2. Estimation of Δ_{canopy} from fluxes and isotopic fluxes

At the leaf level, carbon isotope discrimination has long been used by plant physiologists and ecologists as an indicator of plant carbon and water relations (Farquhar et al., 1989; Ehleringer et al., 1993). A conceptually identical quantity is used at the regional and global scales in large-scale carbon cycle studies that focus on the nature and timing of terrestrial carbon exchange with the atmosphere (Tans et al., 1993; Fung et al., 1997; Battle et al., 2000). Similarly, at the ecosystem-scale, Δ_{canopy} is proving to be a useful parameter in investigations of carbon and water cycling via ecosystem physiological processes (Lloyd

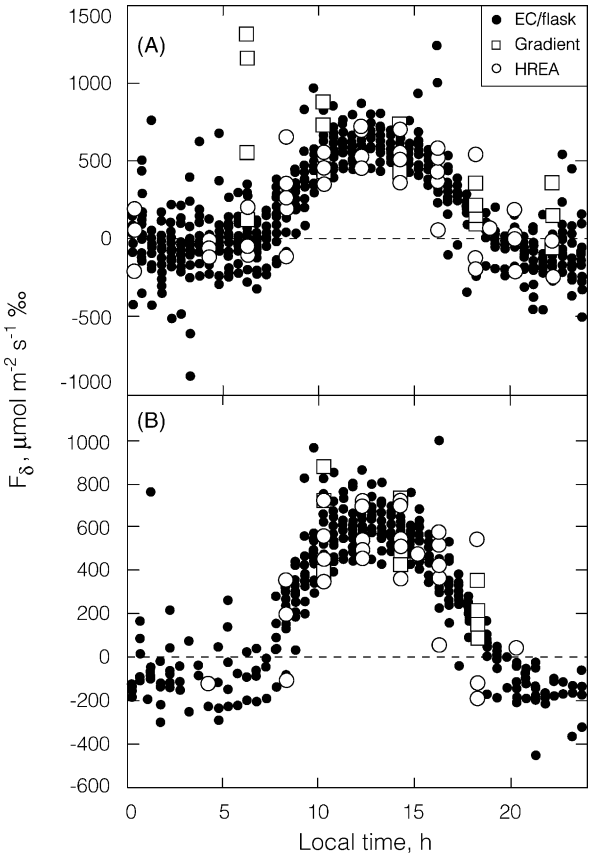

Fig. 5. Diurnal pattern of isotopic flux density (F_δ) measured via EC/flask (filled circles), flux-gradient (empty squares), and HREA (empty circles) methods. Panel (A) shows all data available, which included stationary and non-stationary periods from 11 to 25 August (EC/flask technique) and from 20 to 24 August (gradient and HREA techniques). Panel (B) is a subset of panel (A) but with non-stationary periods removed. Isotopic storage fluxes have been incorporated into F_δ.

et al., 1996; Yakir and Sternberg, 2000; Bowling et al., 2001b; Baldocchi and Bowling, 2003).

Bowling et al. (2001b) showed that flux and isotopic flux measurements such as those in Figs. 3 and 5 can be used to partition F into F_A and F_R using Eqs. (1) and (2). This approach requires an estimate of flux-weighted, whole-canopy integrated photosynthetic discrimination (Δ_{canopy}), which cannot be obtained by direct measurement. In fact, a primary conclusion of Bowling et al. (2001b) was that the isotopic approach to partitioning net ecosystem exchange is quite sensitive to Δ_{canopy}, and thus further exploration of Δ_{canopy} is warranted. In this study, we chose to specify the total ecosystem respiration flux F_R in another fashion, then use Eqs. (1) and (2) to solve for F_A and Δ_{canopy} as unknowns (rather than F_A and F_R as in Bowling et al., 2001b).

A common method to estimate total ecosystem respiration at eddy flux sites is examination of nocturnal F, when photosynthesis is absent (Goulden et al., 1996; Valentini et al., 2000). Since at night the flux is strictly respiratory, an exponential dependence of measured fluxes on temperature (T) is expected (Lloyd and Taylor, 1994). Nighttime F is shown as a function of measured soil T in Fig. 6, along with spatially averaged soil chamber measurements. Despite an 8 °C range in soil T, there was not a clear dependence of either F or chamber respiration measurements on soil T (Fig. 6), even when the chambers were evaluated individually (data not shown). The chamber measurements generally showed higher respiration than did F. Despite the homogenous plant canopy, more spatial variability was evident in the chamber measurements than variability due to T (not shown). We did not measure soil

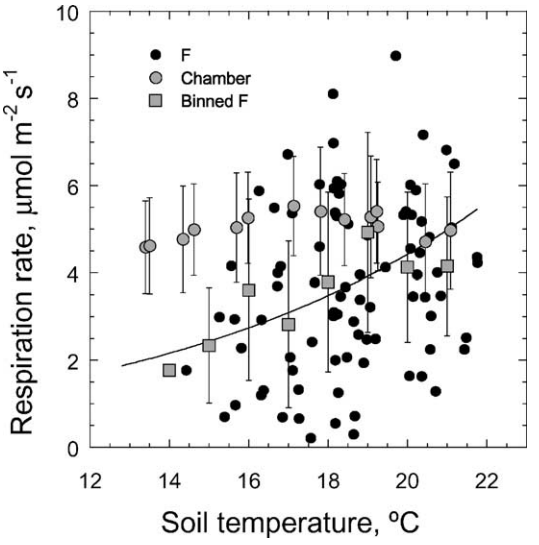

Fig. 6. Respiration as a function of soil temperature (at 0.04 m depth). Data are shown for nocturnal F during stationary periods (filled circles), and for soil chambers measured throughout the diel period (shaded circles). Soil chamber data are spatial averages along a 100 m transect (mean ± S.D.). Also shown are the F data averaged within 1 °C bins (shaded squares, mean ± S.D.). The line is an exponential regression through the binned F data ($F_R(T) = 0.406\, e^{0.119T}$; $r^2 = 0.730$).

moisture along the soil respiration transect, but we did observe variation in volumetric soil moisture (9–13% at 0.15 ± 0.02 m depth) in the soil pits used for organic sample collection. The high degree of spatial variability in soil respiration was likely a consequence of soil moisture variation (Davidson et al., 1998; Law et al., 2001). Since F also includes the foliar component of total ecosystem respiration, it should be larger than soil chamber estimates. We attempted to measure total ecosystem respiration (including the foliage) with chambers, which would have possibly resolved this discrepancy. Unfortunately, this measurement was unsuccessful due to instrument problems in the field.

Only when the nocturnal F data were bin-averaged in 1 °C increments was an exponential relationship apparent (Fig. 6). This is common in eddy flux studies (Greco and Baldocchi, 1996). Since our goal is to examine Δ_{canopy}, we make the assumption that this regression provides an adequate representation of the true total ecosystem respiration flux. We acknowledge that this is a weak assumption. However, it facilitates a comparison with independent isotopic measurements that provide some confidence for our interpretation of Δ_{canopy} and the isotopic content of the photosynthetic flux (below).

Fluxes of F, F_R (defined by the regression), and F_A (where $F_A = F - F_R(T)$) are shown in Fig. 7. $F_R(T)$ peaked in late afternoon (16:00–16:30 h) at about 5 μmol m^{-2} s^{-1}, while the assimilation peak (−30 μmol m^{-2} s^{-1}) occurred earlier (14:00 h). Combining these fluxes with the EC/flask isotopic fluxes of Fig. 5B, specifying $\delta^{13}C_R$ using the Keeling plot (Table 1), and estimating $\delta^{13}C_a$ using measured [CO_2] at 0.4 m (0.8h) and the $\delta^{13}C$ versus 1/[CO_2] regression (Table 1), we can solve for Δ_{canopy} using Eqs. (1) and (2).

The daytime diurnal pattern of Δ_{canopy} is shown in Fig. 8A. There was a general peak of about 19‰ around 11:00 h, and a gradual decrease to near 15‰ at the end of the day. This pattern differs somewhat from the diurnal pattern of discrimination reported by Bowling et al. (2001b) over a deciduous forest, which was similar (19‰) in the early morning, and decreased rapidly to about 17‰ at 12:00 h, then stayed constant until sunset. In their study, Δ_{canopy} was estimated by inverting the Penman–Monteith equation and using a derived canopy conductance. The F-weighted average for Δ_{canopy} in the present study was 17.9‰. This is lower than Δ_e, the ecosystem discrimination defined by Buchmann et al. (1998), which was −19.7‰ for

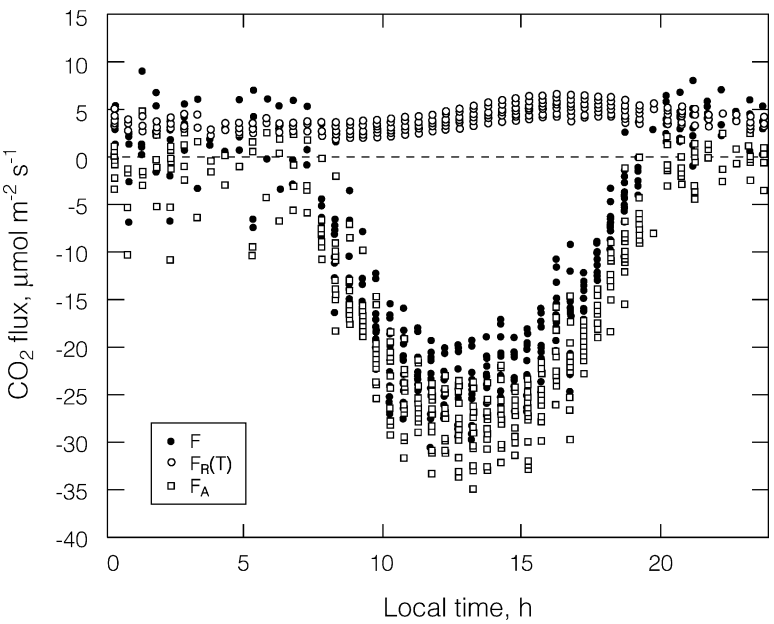

Fig. 7. Diurnal pattern of F (filled circles), respiration (F_R, as a function of T, using the regression shown in Fig. 6, empty circles), and photosynthesis ($F_A = F - F_R(T)$, empty squares) fluxes during stationary periods from 11 to 25 August.

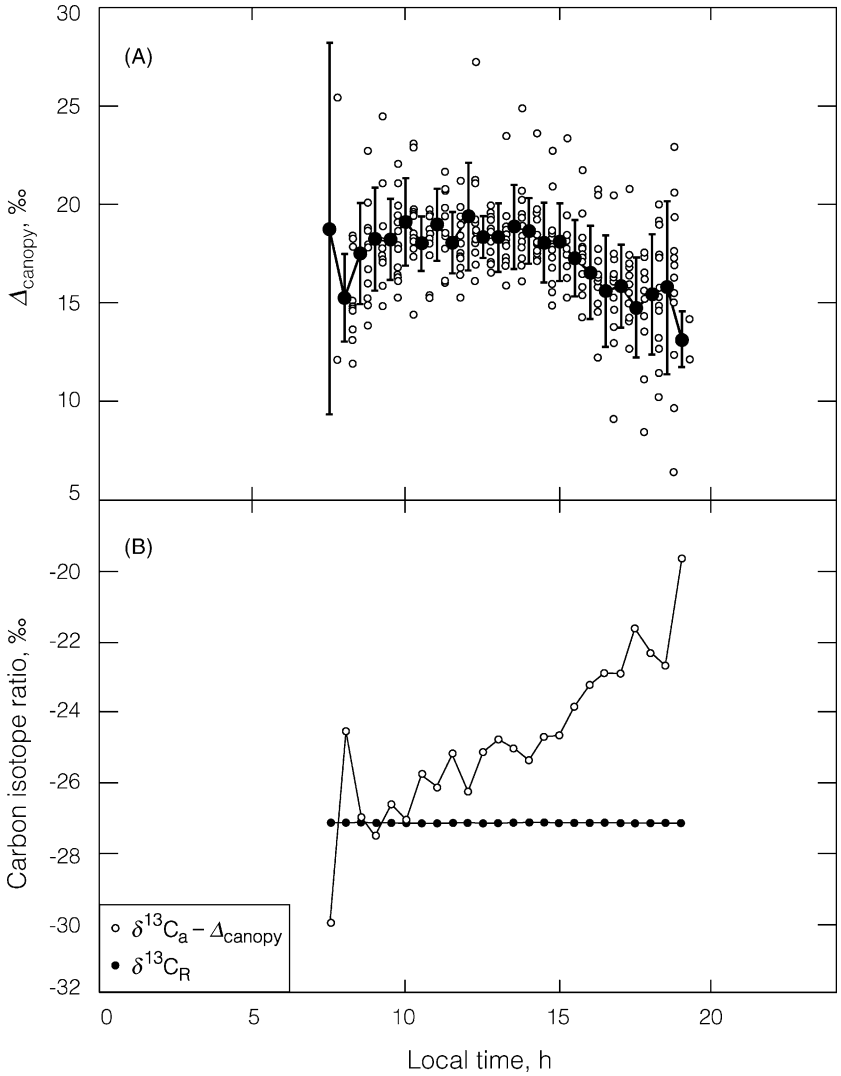

Fig. 8. (A) Whole-canopy carbon isotope discrimination (empty circles), derived using the fluxes in Fig. 7 and the EC/flask estimates of F_δ in Fig. 5B, and Eqs. (1) and (2). Half-hourly means (±S.D.) are also shown (filled circles). Data are shown only for daylight periods ($R_n > 50\,W\,m^{-2}$) when $F_A < -5\,\mu mol\,m^{-2}\,s^{-1}$. (B) The isotopic composition of the photosynthetic flux (empty circles), and of the respired flux (filled circles). The latter was calculated from the Keeling plot (Table 1).

our study using $\delta^{13}C_R$ (Table 1) and the Niwot Ridge isotopic value cited above (−7.92‰) as the free tropospheric value. Δ_{canopy} and Δ_e are different definitions of discrimination and do not represent the same quantity. Δ_{canopy} represents the carbon isotope discrimination associated with net photosynthesis (gross carbon uptake minus leaf respiration), integrated over an entire plant canopy, while Δ_e describes the isotopic influence of ecosystem respiration on the free troposphere.

Using an ecophysiological canopy model, Baldocchi and Bowling (2003) have shown that considerable seasonal variation in Δ_{canopy} can be expected based on the response of photosynthesis and stomatal conductance to environmental variation (in particular light and humidity). Bowling et al. (2002) showed that $\delta^{13}C_R$ varies in response to freezing air temperatures and variations in vapor pressure deficit of air, implying a change in Δ_{canopy} on a scale of days to

weeks. Hence, we expect that our present estimates of Δ_{canopy} may not be representative of a time period of more than several days.

4.1.3. $\delta^{13}C$ of the photosynthetic and respiratory fluxes and organic materials

The quantity $\delta^{13}C_a - \Delta_{canopy}$ in Eq. (2) (which we will call $\delta^{13}C_P$) describes the isotopic composition of carbon removed by the photosynthetic assimilation flux throughout the day. This quantity is shown in Fig. 8B, along with $\delta^{13}C_R$, the isotopic composition of the respiration flux, for comparison. There was a strong diurnal change in $\delta^{13}C_P$, from −27.5‰ at 09:00 h to −22.3‰ at 18:00 h. At isotopic equilibrium, $\delta^{13}C_R = \delta^{13}C_a - \Delta_{canopy}$, and Eq. (2) is simply a multiple of Eq. (1). Equilibrium occurred only very early in the morning, and in fact the *F*-weighted average of $\delta^{13}C_P$ was –25.1‰, a full 2‰ offset from $\delta^{13}C_R$ (Table 1). It is only through this time-varying disequilibrium that Eqs. (1) and (2) can be used as independent equations.

Bowling et al. (2002) showed that there is a link between $\delta^{13}C_R$ and vapor pressure saturation deficit (vpd) of the air, implying indirectly that Δ_{canopy} responds to changes in vpd. The diel pattern of the isotopic composition of the photosynthetic flux ($\delta^{13}C_P$) in Fig. 8B follows the diel pattern in vpd closely, with the most positive $\delta^{13}C_P$ at the end of the day when vpd was the highest. $\delta^{13}C_a$ changed by only 2.4‰ over this time period (from −9.2‰ at 09:00 h to −6.8‰ at 18:00 h, not shown in Fig. 8), which is not enough to account for the full change in $\delta^{13}C_P$. This provides support for the hypothesis that Δ_{canopy} varies on diel time scales in response to environmental variables, possibly through diel changes in stomatal conductance.

The isotopic composition of ecosystem carbon stocks and fluxes is shown in Fig. 9. Sun leaves exhibited the most negative $\delta^{13}C$ (−28.0‰) of all measured samples, and the CO_2 respired from whole branches was the most positive (−23.8‰). (Shade leaves are typically quite negative but they were not measured.) All measured stocks except sun leaves were more enriched than the total respiration flux. There was only marginal isotopic enrichment in bulk SOM with depth, a phenomenon commonly observed in natural soils (e.g. Ehleringer et al., 2000). Since total ecosystem respiration is a combination of soil

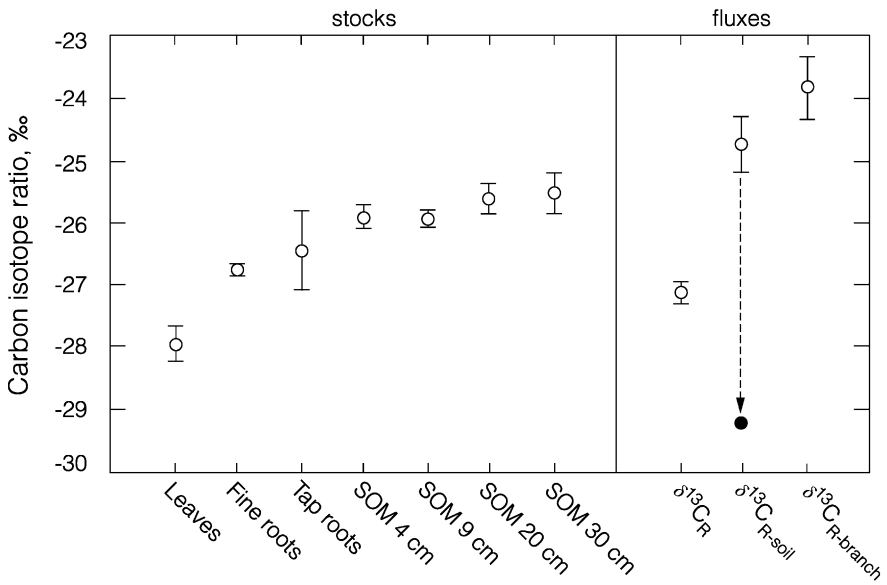

Fig. 9. Isotopic composition of various ecosystem organic components (left panel), and ecosystem fluxes (right panel). Data are means and standard errors (for the organics), or Keeling plot intercepts (Table 1) with error bars equal to the standard error of the intercepts (for the fluxes). The theoretical point (filled circle) is equal to the soil-respired value minus 4.4‰, and represents the maximum possible measurement error associated with disturbance of the isotopically enriched soil gas profile.

respiration (all belowground processes including root respiration) and foliar respiration, we expected that $\delta^{13}C_R$ would fall between the isotopic compositions of the soil-respired and branch-respired fluxes. Conservation of mass dictates that:

$$\delta^{13}C_R(F_R) = \delta^{13}C_{R\text{-soil}}(F_{R\text{-soil}}) + \delta^{13}C_{R\text{-branch}}(F_{R\text{-branch}}), \quad (10)$$

where the subscripts 'R-soil' and 'R-branch' denote the soil-respired and branch-respired fluxes, respectively, and $F_R = F_{R\text{-soil}} + F_{R\text{-branch}}$. However, both component fluxes were more enriched than $\delta^{13}C_R$ (Fig. 9), which violates conservation of mass. We suspect that our soil chamber isotopic measurements might be in error. A pool of enriched CO_2 normally resides in the undisturbed soil profile (Cerling et al., 1991), and a measurement which disturbs this profile could be in error by as much as 4.4‰, the fractionation factor associated with binary diffusion of CO_2 in air. The filled circle in Fig. 9 displays the theoretical lower limit for the soil-respired flux, which is considerably lower than $\delta^{13}C_R$. This is not an issue with the branch-flux measurements since the volume of air where diffusion is dominant is very small.

Perhaps the most important result of our study is the demonstration that $\delta^{13}C$ of ecosystem carbon stocks (leaves, roots, SOM) is a poor predictor of ecosystem carbon fluxes ($\delta^{13}C_P$ and $\delta^{13}C_R$). $\delta^{13}C_P$ was always more enriched than bulk sun leaf tissue, and more enriched than $\delta^{13}C_R$ for the majority of the day. Neither fine roots, tap roots, nor SOM matched $\delta^{13}C_{R\text{-soil}}$, although it is possible that the 4.4‰ error might not be fully expressed.

5. Conclusions

Despite potential problems with each technique, we have demonstrated that the EC/flask, flux-gradient, and HREA methods provide similar estimates of ecosystem isotopic fluxes. Since the EC/flask method is fairly easy to apply, a survey of ecosystem isotope dynamics at a variety of ecosystem eddy flux sites is a realistic and attainable goal. However, these methods remain estimates of ecosystem isotopic fluxes, and are dependent on unresolved assumptions. These assumptions include scalar similarity and well-defined vertical profile relationships for CO_2 and its isotopic forms (HREA and gradient techniques), and validity of the relationship in Fig. 4 at all time scales relevant to turbulent transport (EC/flask technique). Robust determination of isotopic fluxes will require development of instrumentation that can directly measure eddy covariance of $^{13}CO_2$.

The relationship between $\delta^{13}C$ and $[CO_2]$ was consistent except during the morning boundary layer transition, but reasons for this discrepancy are unclear. Values for Δ_{canopy} were obtained that are consistent with other canopy-level studies, and realistic from a leaf-level physiological perspective. The isotopic composition of the assimilation flux ($\delta^{13}C_P$) was not in equilibrium with the respiration flux except in the early morning. $\delta^{13}C_P$ changed over the diel pattern, becoming more enriched at the end of the day when vpd was highest. Finally, the carbon isotope ratio of ecosystem carbon stocks does not appear to be a good predictor of the isotopic content of ecosystem carbon fluxes.

Acknowledgements

Russ Monson provided invaluable scientific and logistical insight in the early stages of this work. Larry Flanagan suggested using the partitioning equations to examine discrimination, and has provided many interesting and useful discussions. Several scientists provided helpful suggestions regarding the terminology in Appendix A. Chun-Ta Lai provided comments on an earlier version of this paper. We are grateful to Ray Cartee and the Utah Agricultural Experiment Station at Utah State University for access to the site, and to Larry Hipps for advice and logistical support. Jean Ometto, Julianna Fessenden, Shannon Kincaid, and Tomas Domingues provided assistance with field work. Craig Cook, Mike Lott, Shannon Kincaid, and Saltbush Bill supplied outstanding isotopic assistance. This material is based upon work supported by the National Science Foundation under Grant No. 9905717. Any opinions, findings, and conclusions or recommendations expressed in this material are those of the author(s) and do not necessarily reflect the views of the National Science Foundation.

Appendix A. Isoflux and net ecosystem exchange of $^{13}CO_2$

Differing terminology in different fields, and in our own papers (Bowling et al., 1999a, 2001b), has led to some confusion in discussions with colleagues about isotopic net exchange fluxes. In particular, the isoflux (Bowling et al., 2001b) is similar in context to net ecosystem exchange of $^{13}CO_2$, but they are not equal. Here we discuss the pertinent equations and introduce terminology that we hope will provide clarity in future analyses of ecosystem net isotopic exchange.

The "iso-" prefix generally refers to a constant quantity in meteorology (e.g. isotherms), analytical chemistry (isoconcentration), and fluid dynamics (isoflux, constant flux). However, these terms are also used in the carbon cycle community to refer to the product of isotopic composition and CO_2 concentration or mole fraction (isoconcentration, Raupach, 2001), or the product of isotopic composition and CO_2 flux (isoflux, Bowling et al., 2001b). These terms, especially isoflux, are common parlance within the global carbon cycle community, but are used more frequently in discussions than in the scientific literature (e.g. Rayner et al., 1999). All scientific approaches that use conservation of mass for total CO_2 and $^{13}CO_2$ use the isoflux concept when the mass conservation for $^{13}CO_2$ is expressed using δ notation (e.g. Tans et al., 1993; Francey et al., 1995; Fung et al., 1997; Bowling et al., 2001b).

Formally, net ecosystem exchange (F) of total CO_2 is described by conservation of mass in a three-dimensional context (e.g. Baldocchi et al., 1988). With appropriate site selection, terms associated with flux divergence and horizontal heterogeneity can be neglected, reducing the description of F to:

$$F = F_c + \frac{dC_a}{dt} = F_R + F_A, \tag{A.1}$$

where F_c is total CO_2 flux density (measured by eddy covariance), and dC_a/dt is the storage flux density, which is the time rate of change of CO_2 mole fraction (C_a) within the canopy between ground level and the measurement height, both expressed on a ground area basis (μmol CO_2 m^{-2} s^{-1}). Eq. (A.1) applies to a suitable control volume where spatial averaging masks any localized near-field effects (Raupach, 1989). F can be interpreted in a biological context (on the right hand side of Eq. (A.1)) as the sum of the CO_2 flux densities of total ecosystem respiration (F_R) and photosynthetic assimilation (F_A), where F_A is negative.

Multiplying each term in Eq. (A.1) by its respective isotope ratio, we obtain an expression for the net ecosystem exchange of $^{13}CO_2$:

$$R_c F_c + \frac{d(R_a C_a)}{dt} = R_R F_R + R_P F_A, \tag{A.2}$$

where the R terms are the molar isotope ratios of the net flux (R_c), the air within the canopy (R_a), the respiratory flux (R_R), and the CO_2 removed by photosynthesis (R_P, subscript 'P' is used to avoid confusion with R_a). When the isotope ratios are expressed as $^{13}C/(^{12}C + {}^{13}C)$, Eq. (A.2) is exactly equal to the net ecosystem exchange of $^{13}CO_2$. When standard ($^{13}C/^{12}C$) isotope ratios are used, a small error is introduced (Bowling et al., 2001b).

Following the leaf level definitions of Farquhar et al. (1989), we now define a whole-canopy, flux-weighted photosynthetic fractionation factor α_{canopy} as the ratio of the molar isotope ratios of air (R_a) and photosynthate (R_P):

$$\alpha_{canopy} = \frac{R_a}{R_P}, \tag{A.3}$$

and substitute into Eq. (A.2) to obtain:

$$F_{13} = R_c F_c + \frac{d(R_a C_a)}{dt} = R_R F_R + \frac{R_a}{\alpha_{canopy}} F_A. \tag{A.4}$$

This equation represents conservation of mass for $^{13}CO_2$, and states that the net ecosystem exchange of $^{13}CO_2$ (denoted F_{13}) is equal to the sum of a flux term ($R_c F_c$) and a storage term ($d(R_a C_a)/dt$). On the RHS of Eq. (A.4), the $^{13}CO_2$ produced by total ecosystem respiration is equal to the product of the isotope ratio of the respiration flux (R_R) times the flux (F_R), and the $^{13}CO_2$ removed by photosynthesis is the product of the isotope ratio of the photosynthate produced (R_P) and the photosynthetic flux (F_A). R_P reflects both the isotopic composition of the air (R_a) and the fractionation associated with carbon isotope discrimination by photosynthesis (α_{canopy}). We can convert this relationship to common isotopic notation making use of standard definitions for isotopic composition ($\delta^{13}C$) and discrimination (Δ;

Farquhar et al., 1989):

$$\delta^{13}\mathrm{C} = \left(\frac{R_\mathrm{m}}{R_\mathrm{PDB}} - 1\right) 1000, \tag{A.5}$$

$$\Delta_\mathrm{canopy} = (\alpha_\mathrm{canopy} - 1)1000, \tag{A.6}$$

where the molar ratio of the sample and isotopic standard are R_m and R_PDB, respectively. Eq. (A.6) in our context represents the discrimination associated with the entire canopy. Dividing Eq. (A.4) through by R_PDB and substituting Eq. (A.6):

$$\frac{R_\mathrm{c}}{R_\mathrm{PDB}} F_\mathrm{c} + \frac{\mathrm{d}}{\mathrm{d}t}\left(\frac{R_\mathrm{a}}{R_\mathrm{PDB}} C_\mathrm{a}\right) = \frac{R_\mathrm{R}}{R_\mathrm{PDB}} F_\mathrm{R} + \frac{R_\mathrm{a}}{R_\mathrm{PDB}}\left(\frac{1}{(\Delta_\mathrm{canopy}/1000) + 1}\right) F_\mathrm{A}. \tag{A.7}$$

This equation can be reduced to:

$$\underbrace{\left(\frac{\delta_\mathrm{c}}{1000} F_\mathrm{c} + \frac{\mathrm{d}}{\mathrm{d}t}\left(\frac{\delta_\mathrm{a}}{1000} C_\mathrm{a}\right)\right)}_{\mathrm{I}} + \underbrace{\left(F_\mathrm{c} + \frac{\mathrm{d}C_\mathrm{a}}{\mathrm{d}t}\right)}_{\mathrm{II}} = \underbrace{\left(\frac{\delta_\mathrm{R}}{1000} F_\mathrm{R} + \frac{\delta_\mathrm{a} - \Delta_\mathrm{canopy}}{1000} F_\mathrm{A}\right)}_{\mathrm{III}} + \underbrace{(F_\mathrm{R} + F_\mathrm{A})}_{\mathrm{IV}}, \tag{A.8}$$

by neglecting the intermediate terms $(\Delta_\mathrm{canopy}/1000)^2$ and $\Delta_\mathrm{canopy}\delta_\mathrm{a}/(1000)^2$. In Eq. (A.8), terms II and IV are equal (Eq. (A.1)), so they can be subtracted away to obtain:

$$\delta_\mathrm{c} F_\mathrm{c} + \frac{\mathrm{d}(\delta_\mathrm{a} C_\mathrm{a})}{\mathrm{d}t} = \delta_\mathrm{R} F_\mathrm{R} + (\delta_\mathrm{a} - \Delta_\mathrm{canopy}) F_\mathrm{A}. \tag{A.9}$$

Eq. (A.9) is simply the delta-notation form of Eq. (A.4).

We summarize the three relevant equations here. Net ecosystem exchange is expressed for total CO_2 as:

$$F = F_\mathrm{c} + \frac{\mathrm{d}C_\mathrm{a}}{\mathrm{d}t} = F_\mathrm{R} + F_\mathrm{A}, \tag{A.10}$$

and is expressed for $^{13}CO_2$ as:

$$F_{13} = R_\mathrm{c} F_\mathrm{c} + \frac{\mathrm{d}(R_\mathrm{a} C_\mathrm{a})}{\mathrm{d}t} = R_\mathrm{R} F_\mathrm{R} + \frac{R_\mathrm{a}}{\alpha} F_\mathrm{A}. \tag{A.11}$$

In common isotopic notation, Eq. (A.11) is expressed as an isoflux (F_δ):

$$F_\delta = \delta_\mathrm{c} F_\mathrm{c} + \frac{\mathrm{d}(\delta_\mathrm{a} C_\mathrm{a})}{\mathrm{d}t} = \delta_\mathrm{R} F_\mathrm{R} + (\delta_\mathrm{a} - \Delta_\mathrm{canopy}) F_\mathrm{A}. \tag{A.12}$$

These equations show that the net exchange terms in each (F, F_{13}, F_δ) are defined (in a measurement context) as the sum of a flux density term (F_c, $R_\mathrm{c}F_\mathrm{c}$, $\delta_\mathrm{c}F_\mathrm{c}$) and a storage flux density term ($\mathrm{d}C_\mathrm{a}/\mathrm{d}t$, $\mathrm{d}(R_\mathrm{a}C_\mathrm{a})/\mathrm{d}t$, $\mathrm{d}(\delta_\mathrm{a}C_\mathrm{a})/\mathrm{d}t$). Each net exchange term comprises (in a biological context) a respiration term (F_R, $R_\mathrm{R}F_\mathrm{R}$, $\delta_\mathrm{R}F_\mathrm{R}$) and a photosynthetic assimilation term (F_A, $R_\mathrm{a}F_\mathrm{A}/\alpha$, $(\delta_\mathrm{a} - \Delta_\mathrm{canopy})F_\mathrm{A}$). F_{13} is equal to the net ecosystem exchange of $^{13}CO_2$, and the isoflux (F_δ) has the same conceptual meaning but is mathematically distinct. Hence, we use the subscripts on the isotopic net exchange terms (F_{13}, F_δ) to describe the form in which the equation is expressed. Measurements of net isotopic exchange may be expressed in either form, with appropriate units. Eq. (A.10) can be combined with either Eq. (A.11) or (A.12) to describe the relationships between net ecosystem exchange (F, F_{13}, F_δ) and biological processes (F_A, F_R, Δ_canopy). Formally, the isoflux (F_δ) is an isotopic flux density, with units of $\mu\mathrm{mol\,m^{-2}\,s^{-1}}$ ‰.

Bowling et al. (2001b) expressed Eqs. (A.10) and (A.12) as:

$$\mathrm{NEE} = F_\mathrm{R} + F_\mathrm{A}, \tag{A.13}$$

$$\mathrm{isoflux} = \delta^{13}\mathrm{C}_\mathrm{R}(F_\mathrm{R}) + (\delta^{13}\mathrm{C}_\mathrm{a} - \Delta) F_\mathrm{A}. \tag{A.14}$$

However, we recommend using the notation in Eqs. (A.10), (A.11) and (A.12) for clarity.

The sign of the net isotopic exchange terms (F_{13}, F_δ) is important. Our convention is that fluxes directed away from the canopy are positive, and so during photosynthetic periods F and F_{13} are negative. However, the arbitrary use of PDB as the isotopic ^{13}C standard forces F_δ to be positive during CO_2 uptake.

References

Asseng, S., Hsiao, T.C., 2000. Canopy CO_2 assimilation, energy balance, and water use efficiency of an alfalfa crop before and after cutting. Field Crops Res. 67, 191–206.

Baldocchi, D.D., Bowling, D.R., 2003. Modeling the discrimination of $^{13}CO_2$ above and within a temperate broad-leaved forest canopy on hourly to seasonal time scales. Plant Cell Environ. 26, 231–244.

Baldocchi, D.D., Hicks, B.B., Meyers, T.P., 1988. Measuring biosphere–atmosphere exchanges of biologically related gases with micrometeorological methods. Ecology 69, 1331–1340.

Battle, M., Bender, M.L., Tans, P.P., White, J.W.C., Ellis, J.T., Conway, T., Francey, R.J., 2000. Global carbon sinks and their variability inferred from atmospheric O_2 and $\delta^{13}C$. Science 287, 2467–2470.

Becker, J.F., Sauke, T.B., Loewenstein, M., 1992. Stable isotope analysis using tunable diode laser spectroscopy. Appl. Opt. 31, 1921–1927.

Bowling, D.R., Turnipseed, A.A., Delany, A.C., Baldocchi, D.D., Greenberg, J.P., Monson, R.K., 1998. The use of relaxed eddy accumulation to measure biosphere–atmosphere exchange of isoprene and other biological trace gases. Oecologia 116, 306–315.

Bowling, D.R., Baldocchi, D.D., Monson, R.K., 1999a. Dynamics of isotopic exchange of carbon dioxide in a Tennessee deciduous forest. Global Biogeochem. Cycles 13, 903–922.

Bowling, D.R., Delany, A.C., Turnipseed, A.A., Baldocchi, D.D., Monson, R.K., 1999b. Modification of the relaxed eddy accumulation technique to maximize measured scalar mixing ratio differences in updrafts and downdrafts. J. Geophys. Res. 104, 9121–9133.

Bowling, D.R., Cook, C.S., Ehleringer, J.R., 2001a. Technique to measure CO_2 mixing ratio in small flasks with a bellows/IRGA system. Agric. For. Meteorol. 109, 61–65.

Bowling, D.R., Tans, P.P., Monson, R.K., 2001b. Partitioning net ecosystem carbon exchange with isotopic fluxes of CO_2. Global Change Biol. 7, 127–145.

Bowling, D.R., McDowell, N.G., Bond, B.J., Law, B.E., Ehleringer, J.R., 2002. ^{13}C content of ecosystem respiration is linked to precipitation and vapor pressure deficit. Oecologia 131, 113–124.

Brakke, T.W., Verma, S.B., Rosenberg, N.J., 1978. Local and regional components of sensible heat advection. J. Appl. Meteorol. 17, 955–963.

Buchmann, N., Ehleringer, J.R., 1998. CO_2 concentration profiles, and carbon and oxygen isotopes in C_3 and C_4 crop canopies. Agric. For. Meteorol. 89, 45–58.

Buchmann, N., Kao, W.-Y., Ehleringer, J., 1997. Influence of stand structure on carbon-13 of vegetation, soils, and canopy air within deciduous and evergreen forests in Utah, United States. Oecologia 110, 109–119.

Buchmann, N., Brooks, J.R., Flanagan, L.B., Ehleringer, J.R., 1998. Carbon isotope discrimination of terrestrial ecosystems. In: Griffiths, H. (Ed.), Stable Isotopes, Integration of Biological, Ecological, and Geochemical Processes. BIOS Scientific Publishers, Oxford, 438 pp.

Businger, J.A., 1986. Evaluation of the accuracy with which dry deposition can be measured with current micrometeorological techniques. J Clim. Appl. Meteorol. 25, 1100–1124.

Businger, J.A., Oncley, S.P., 1990. Flux measurement with conditional sampling. J. Atmos. Oceanic Technol. 7, 349–352.

Cellier, P., Brunet, Y., 1992. Flux-gradient relationships above tall plant canopies. Agric. For. Meteorol. 58, 93–117.

Cerling, T.E., Solomon, D.K., Quade, J., Bowman, J.R., 1991. On the isotopic composition of carbon in soil carbon dioxide. Geochim. Cosmochim. Acta 55, 3403–3405.

Crosson, E.R., et al., 2002. Stable isotope ratios using cavity ringdown spectroscopy: determination of $^{13}C/^{12}C$ for carbon dioxide in human breath. Anal. Chem. 74, 2003–2007.

Davidson, E.A., Belk, E., Boone, R.D., 1998. Soil water content and temperature as independent or confounded factors controlling soil respiration in a temperate mixed hardwood forest. Global Change Biol. 4, 217–227.

Denmead, O.T., Bradley, E.F., 1985. Flux-gradient relationships in a forest canopy. In: Hutchinson, B.A., Hicks, B.B. (Eds.), The Forest–Atmosphere Interaction. Reidel, Norwell, MA, pp. 421–442.

Duranceau, M., Ghashghaie, J., Badeck, F.-W, Deleens, E., Cornic, G., 1999. $\delta^{13}C$ of CO_2 respired in the dark in relation to $\delta^{13}C$ of leaf carbohydrates in *Phaseolus vulgaris* L. under progressive drought. Plant Cell Environ. 22, 515–523.

Ehleringer, J.R., Cook, C.S., 1998. Carbon and oxygen isotope ratios of ecosystem respiration along an Oregon conifer transect: preliminary observations based on small-flask sampling. Tree Physiol. 18, 513–519.

Ehleringer, J.R., Hall, A.E., Farquahar, G.D. (Eds), 1993. Stable Isotopes and Plant Carbon–Water Relations. Academic Press, San Diego, 555 pp.

Ehleringer, J.R., Buchmann, N., Flanagan, L.B., 2000. Carbon isotope ratios in belowground carbon cycle processes. Ecol. Appl. 10, 412–422.

Esler, M.B., Griffith, D.W.T., Wilson, S.R., Steele, L.P., 2000. Precision trace gas analysis by FT-IR spectroscopy. 2. The $^{13}C/^{12}C$ isotope ratio of CO_2. Anal. Chem. 72, 216–221.

Farquhar, G.D., Ehleringer, J.R., Hubick, K.T., 1989. Carbon isotope discrimination and photosynthesis. Annu. Rev. Physiol. Plant Mol. Biol. 40, 503–537.

Flanagan, L.B., Brooks, J.R., Varney, G.T., Berry, S.C., Ehleringer, J.R., 1996. Carbon isotope discrimination during photosynthesis and the isotope ratio of respired CO_2 in boreal forest ecosystems. Global Biogeochem. Cycles 10, 629–640.

Flanagan, L.B., Brooks, J.R., Varney, G.T., Ehleringer, J.R., 1997. Discrimination against $C^{18}O^{16}O$ during photosynthesis and the oxygen isotope ratio of respired CO_2 in boreal forest ecosystems. Global Biogeochem. Cycles 11, 83–98.

Flesch, T.K., Prueger, J.H., Hatfield, J.L., 2002. Turbulent Schmidt number from a tracer experiment. Agric. For. Meteorol. 111, 299–307.

Foken, T., Wichura, B., 1996. Tools for quality assessment of surface-based flux measurements. Agric. For. Meteorol. 78, 83–105.

Francey, R.J., Tans, P.P., Allison, C.E., Enting, I.G., White, J.W.C., Trolier, M., 1995. Changes in oceanic and terrestrial uptake since 1982. Nature 373, 326–330.

Fung, I., Field, C.B., Berry, J.A., Thompson, M.V., Randerson, J.T., Malmström, C.M., Vitousek, P.M., Collatz, G.J., Sellers, P.J., Randall, D.A., Denning, A.S., Badeck, F.-W, John, J., 1997. Carbon-13 exchanges between the atmosphere and the biosphere. Global Biogeochem. Cycles 11, 507–533.

Ghashghaie, J., Duranceau, M., Badeck, F.-W., Cornic, G., Adeline, M.-T., Deleens, E., 2001. $\delta^{13}C$ of CO_2 respired in the dark in relation to $\delta^{13}C$ of leaf metabolites: comparison between *Nicotiana sylvestris* and *Helianthus annuus* under drought. Plant Cell Environ. 24, 505–515.

Gleixner, G., Scrimgeour, C., Schmidt, H.-L., Viola, R., 1998. Stable isotope distribution in the major metabolites of source and sink organs of *Solanum tuberosum* L.: a powerful tool in the study of metabolic partitioning in intact plants. Planta 207, 241–245.

Goulden, M.L., Munger, J.W., Fan, S.-M., Daube, B.C., Wofsy, S.C., 1996. Measurements of carbon sequestration by long-term eddy covariance: methods and a critical evaluation of accuracy. Global Change Biol. 2, 169–182.

Greco, S., Baldocchi, D.D., 1996. Seasonal variations of CO_2 and water vapour exchange rates over a temperate deciduous forest. Global Change Biol. 2, 183–197.

Henn, M.R., Chapela, I.H., 2000. Differential C isotope discrimination by fungi during decomposition of C_3- and C_4-derived sucrose. Appl. Environ. Microbiol. 66, 4180–4186.

Kaimal, J.C., Finnigan, J.J., 1994. Atmospheric Boundary Layer Flows, Their Structure and Measurement. Oxford University Press, New York, 289 pp.

Keeling, C.D., 1958. The concentrations and isotopic abundances of atmospheric carbon dioxide in rural areas. Geochim. Cosmochim. Acta 13, 322–334.

Law, B.E., Kelliher, F.M., Baldocchi, D.D., Anthoni, P.M., Irvine, J., Moore, D., Van Tuyl, S., 2001. Spatial and temporal variation in respiration in a young ponderosa pine forest during a summer drought. Agric. For. Meteorol. 110, 27–43.

Lin, G., Ehleringer, J.R., 1997. Carbon isotopic fractionation does not occur during dark respiration in C_3 and C_4 plants. Plant Physiol. 114, 391–394.

Lloyd, J., Taylor, J.A., 1994. On the temperature dependence of soil respiration. Funct. Ecol. 8, 315–323.

Lloyd, J., Krujit, B., Hollinger, D.Y., Grace, J., Francey, R., Wong, S.-C., Kelliher, F.M., Miranda, A.C., Farquhar, G.D., Gash, J.H.C., Vygodskaya, N.N., Wright, I.R., Miranda, H.S., Schulze, E.-D., 1996. Vegetation effects on the isotopic composition of atmospheric CO_2 at local and regional scales: theoretical aspects and a comparison between rain forest in Amazonia and a boreal forest in Siberia. Aust. J. Plant Physiol. 23, 371–399.

Lloyd, J., Francey, R.J., Mollicone, D., Raupach, M.R., Sogachev, A., Arneth, A., Byers, J.N., Kelliher, F.M., Rebmann, C., Valentini, R., Wong, S.-C., Bauer, G., Schulze, E.-D., 2001. Vertical profiles, boundary layer budgets, and regional flux estimates for CO_2 and its $^{13}C/^{12}C$ ratio and for water vapor above a forest/bog mosaic in central Siberia. Global Biogeochem. Cycles 15, 267–284.

McMillen, R.T., 1988. An eddy correlation technique with extended applicability to non-simple terrain. Boundary Layer Meteorol. 43, 231–245.

Ometto, J.P.H.B., Flanagan, L.B., Martinelli, L.A., Moreira, M.Z., Higuchi, N., Ehleringer, J.R., 2002. Carbon isotope discrimination in forest and pasture ecosystems of the Amazon Basin, Brazil. Global Biogeochem. Cycles 16, 1109, doi: 10-1029/2001GB001462.

Oncley, S.P., Delany, A.C., Horst, T.W., Tans, P.P., 1993. Verification of flux measurement using relaxed eddy accumulation. Atmos. Environ. 27A, 2417–2426.

Pataki, D.E., Ehleringer, J.R., Flanagan, L.B., Yakir, D., Bowling, D.R., Still, C.J., Buchmann, N., Kaplan, J.O., Berry, J.A., 2003. The application and interpretation of Keeling plots in terrestrial carbon cycle research. Global Biogeochem. Cycles, in press.

Quay, P., King, S., Wilbur, D., Wofsy, S., Richey, J., 1989. $^{13}C/^{12}C$ of atmospheric CO_2 in the Amazon Basin: forest and river sources. J. Geophys. Res. 94, 18,327–18,336.

Raupach, M.R., 1979. Anomalies in flux-gradient relationships over forest. Boundary Layer Meteorol. 16, 467–486.

Raupach, M.R., 1989. Applying Lagrangian fluid mechanics to infer scalar source distributions from concentration profiles in plant canopies. Agric. Forest. Meteorol. 47, 85–108.

Raupach, M.R., 2001. Inferring biogeochemical sources and sinks from atmospheric concentrations: general considerations and applications in vegetation canopies. In: Schulze, E.-D., Heimann, M., Harrison, S., Holland, E., Lloyd, J., Prentice, I.C., Schimel, D.S. (Eds.), Global Biogeochemical Cycles in the Climate System. Academic Press, San Diego.

Rayner, P.J., Enting, I.G., Francey, R.J., Langenfelds, R., 1999. Reconstructing the recent carbon cycle from atmospheric CO_2, $\delta^{13}C$, and O_2/N_2 observations. Tellus 51B, 213–232.

Rosenberg, N.J., Verma, S.B., 1978. Extreme evapotranspiration by irrigated alfalfa: a consequence of the 1976 midwestern drought. J. Appl. Meteorol. 17, 934–941.

Ruppert, J., 2002. Eddy sampling methods for the measurement of trace gas fluxes. Masters thesis, Department of Micrometeorology, University of Bayreuth.

Shaw, R.H., 1985. On diffusive and dispersive fluxes in forest canopies. In: Hutchinson, B.A., Hicks, B.B. (Eds.), The Forest–Atmosphere Interaction. Reidel, Norwell, MA, pp. 407–419.

Tans, P.P., Berry, J.A., Keeling, R.F., 1993. Oceanic $^{13}C/^{12}C$ observations: a new window on ocean CO_2 uptake. Global Biogeochem. Cycles 7, 353–368.

Valentini, R., et al., 2000. Respiration as the main determinant of carbon balance in European forests. Nature 404, 861–865.

Verma, S.B., Rosenberg, N.J., 1976. Carbon dioxide concentration and flux in a large agricultural region of the Great Plains of North America. J. Geophys. Res. 81, 399–405.

Webb, E.K., Pearman, G.I., Leuning, R., 1980. Correction of flux measurements for density effects due to heat and water vapour transfer. Q. J. R. Meteorol. Soc. 106, 85–100.

Wofsy, S.C., Goulden, M.L., Munger, J.W., Fan, S.-M., Bakwin, P.S., Daube, B.C., Bassow, S.L., Bazzaz, F.A., 1993. Net exchange of CO_2 in a mid-latitude forest. Science 260, 1314–1317.

Yakir, D., Sternberg, L.S.L., 2000. The use of stable isotopes to study ecosystem gas exchange. Oecologia 123, 297–311.

Yakir, D., Wang, X.-F., 1996. Fluxes of CO_2 and water between terrestrial vegetation and the atmosphere estimated from isotope measurements. Nature 380, 515–517.